Archival Report

Biological Psychiatry: CNNI

Machine Learning Identifies Large-Scale Reward-Related Activity Modulated by Dopaminergic Enhancement in Major Depression

Yuelu Liu, Roee Admon, Monika S. Mellem, Emily L. Belleau, Roselinde H. Kaiser, Rachel Clegg, Miranda Beltzer, Franziska Goer, Gordana Vitaliano, Parvez Ahammad, and Diego A. Pizzagalli

ABSTRACT

BACKGROUND: Theoretical models have emphasized systems-level abnormalities in major depressive disorder (MDD). For unbiased yet rigorous evaluations of pathophysiological mechanisms underlying MDD, it is critically important to develop data-driven approaches that harness whole-brain data to classify MDD and evaluate possible normalizing effects of targeted interventions. Here, using an experimental therapeutics approach coupled with machine learning, we investigated the effect of a pharmacological challenge aiming to enhance dopaminergic signaling on whole-brain response to reward-related stimuli in MDD.

METHODS: Using a double-blind, placebo-controlled design, we analyzed functional magnetic resonance imaging data from 31 unmedicated MDD participants receiving a single dose of 50 mg amisulpride ($MDD_{Amisulpride}$), 26 MDD participants receiving placebo ($MDD_{Placebo}$), and 28 healthy control subjects receiving placebo ($HC_{Placebo}$) recruited through two independent studies. An importance-guided machine learning technique for model selection was used on whole-brain functional magnetic resonance imaging data probing reward anticipation and consumption to identify features linked to MDD ($MDD_{Placebo}$ vs. $HC_{Placebo}$) and dopaminergic enhancement ($MDD_{Amisulpride}$ vs. $MDD_{Placebo}$).

RESULTS: Highly predictive classification models emerged that distinguished $MDD_{Placebo}$ from $HC_{Placebo}$ (area under the curve = 0.87) and $MDD_{Placebo}$ from $MDD_{Amisulpride}$ (area under the curve = 0.89). Although reward-related striatal activation and connectivity were among the most predictive features, the best truncated models based on whole-brain features were significantly better relative to models trained using striatal features only.

CONCLUSIONS: Results indicate that in MDD, enhanced dopaminergic signaling restores abnormal activation and connectivity in a widespread network of regions. These findings provide new insights into the pathophysiology of MDD and pharmacological mechanism of antidepressants at the system level in addressing reward processing deficits among depressed individuals.

Keywords: Biomarker, Biotypes, Depression, Dopamine, fMRI, Machine learning

https://doi.org/10.1016/j.bpsc.2019.10.002

Major depressive disorder (MDD) is a debilitating disorder, often characterized by anhedonia (1), which is poorly addressed by current treatments (1,2). Converging evidence across species suggests that mesocorticolimbic dopaminergic pathways involving the striatum are essential for reward processing (3–5). Dysfunction in this circuit has been associated with deficits in reward processing across psychiatric diseases (6). In MDD, neuroimaging studies have documented decreased striatal activation and reduced functional connectivity between the striatum and other nodes of the brain reward system in response to reward-related stimuli (7–9). Notably, some of these abnormalities were found to be restored in the short term by pharmacologically induced dopaminergic enhancement (10).

Despite advancements in our understanding of the pathophysiology of MDD, an unresolved issue is how enhanced dopaminergic signaling might modulate large-scale whole-brain activation and functional coordination in MDD. Besides the striatum, other brain regions, including the orbitofrontal cortex, amygdala, and anterior cingulate cortex (ACC), have been implicated in reward processing (11–14). Given that antidepressant treatments aiming to increase dopaminergic signaling might have faster therapeutic onsets (15,16), it is important to investigate the effects of dopaminergic enhancement to better understand the potential neural mechanism through which these interventions may address reward processing deficits in MDD. Thus, we identified several needs to address in this study, including developing and evaluating 1) a robust, data-driven, multivariate approach to analyze whole-brain data to probe the purported distributed nature of the reward system, 2) an approach to assess

SEE COMMENTARY ON PAGE 133

ISSN: 2451-9022 Biological Psychiatry: Cognitive Neuroscience and Neuroimaging February 2020; 5:163–172 www.sobp.org/BPCNNI

MDD-related abnormalities and putative normalization of those abnormalities, and 3) comparisons between a multivariate approach and a hypothesis-driven approach to evaluate whether a broad set of regions beyond the striatum does indeed better highlight reward-related abnormalities.

Toward these goals, we used a machine learning–based approach to analyze whole-brain functional magnetic resonance imaging (fMRI) data collected from a double-blind, placebo-controlled study, in which unmedicated individuals with MDD and healthy control subjects (HCs) performed a monetary incentive delay (MID) task after being randomized to either a single low dose of amisulpride (50 mg) or placebo. Amisulpride, a selective dopamine D_2/D_3 receptor antagonist, was selected because of its high affinity to block presynaptic autoreceptors at lower doses, thereby increasing dopamine release (17). In a first step, to identify the effects of enhanced dopaminergic transmission on reward-related brain activity, whole-brain fMRI data were entered into an importance-guided model selection procedure (based on the logistic regression with elastic net regularization) (Figure 1) to identify brain regions in which reward-related metrics were most predictive of differences between the MDD individuals receiving amisulpride versus placebo. Next, to investigate the potential normalizing effect of enhanced dopaminergic transmission on MDD-related abnormalities, brain regions from the previous step were compared with those most predictive of differences between MDD and HC group receiving placebo. The regions with MDD-related abnormalities that also demonstrated an MDD amisulpride effect constitute a potential multivariate signature that we used to assess amisulpride-induced blood oxygen level–dependent (BOLD) normalization in subjects with MDD. Based on prior findings (7,10,18–22), we hypothesized that 1) under placebo, MDD would be associated with widespread reward-related abnormalities along the brain's reward pathway and 2) transient dopamine enhancement would rescue such abnormalities. We further compared whole-brain and hypothesis-driven approaches.

METHODS AND MATERIALS

Participants

Participants were recruited by the Center for Depression, Anxiety and Stress Research at McLean Hospital using online advertisements, mailing, and flyers within the Boston metropolitan areas for two independent studies using identical procedures that each enrolled individuals with MDD and HCs.

Across the first (ClinicalTrials.gov identifier: NCT01253421) and second (NCT01701258) studies, 62 unmedicated individuals with MDD (34 randomized to amisulpride [$MDD_{Amisulpride}$], 28 randomized to placebo [$MDD_{Placebo}$]) and 63 demographically matched HCs ($HC_{Placebo}$: $n = 30$; $HC_{Amisulpride}$: $n = 33$) were run in the imaging session. For the current analyses, we focused on analyses aiming at classifying case versus controls ($MDD_{Placebo}$ vs. $HC_{Placebo}$ model) and classifying the potential normalizing effects of dopaminergic enhancement ($MDD_{Placebo}$ vs. $MDD_{Amisulpride}$ model); thus, 92 participants were considered. Among these 92, 85 had useable fMRI data (participants included in final analysis included $MDD_{Amisulpride}$: $n = 31$; $MDD_{Placebo}$: $n = 26$; $HC_{Placebo}$: $n = 28$). A subset of participants (46 MDD, 23 randomized to amisulpride, 23 to placebo; 20 HC controls randomized to placebo) were included in a recent study that used a region-of-interest (ROI) approach to probe the effects of MDD and amisulpride on striatal activation and functional connectivity (10). Groups were matched for age, gender, ethnicity, and years of education (Table 1). General inclusion criteria were right-handedness, age between 18 and 45 years, no MRI contraindications, no lifetime substance dependence, no past-year substance abuse, and no serious medical conditions. For the MDD groups, a diagnosis of MDD according to the

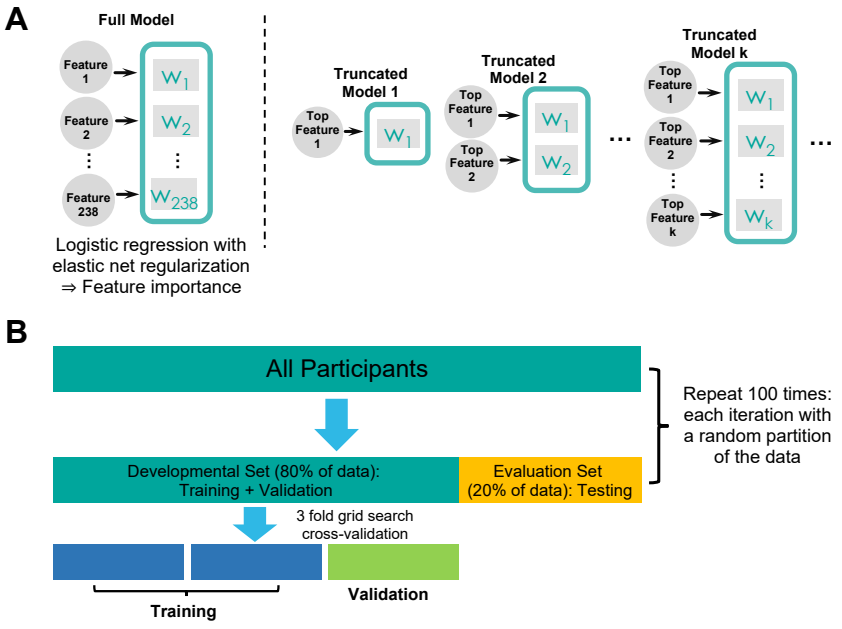

Figure 1. **(A)** An illustration of the importance-guided sequential model selection procedure used to find the optimal set of features. First, a full model including all features is trained using logistic regression with elastic net regularization to determine relative importance of individual features. Next, a series of truncated models were trained based on a progressively increasing set of top features rank ordered by the full model. The set of features in the best truncated model on the evaluation set were deemed as the optimal feature set. **(B)** An illustration of the nested cross-validation procedure used to train, validate, and test the models. A grid search procedure with threefold cross-validation was implemented on the developmental set to determine the best model parameters. The resulting model was further tested on the evaluation set, which contained an independent set of participants *not* used in training and validation. The entire procedure was repeated on 100 different random partitioning of the data to allow for stable model performance. w_i refers to regression weight for feature *i* in the model.

Table 1. Clinical and Demographic Characteristics of the Participants

	$MDD_{Amisulpride}$ ($n = 31$)		$MDD_{Placebo}$ ($n = 26$)		$HC_{Placebo}$ ($n = 28$)	
Characteristic	Mean	SD	Mean	SD	Mean	SD
Age, Years	27.2	7.7	25.6	5.0	25.1	6.1
Education, Years	15.4	2.2	16.8	3.0	15.2	2.9
Beck Depression Inventory-II	26.3	7.9	26.7	7.9	1.8	2.7
Hamilton Depression Rating Scale	15.6	3.7	16.7	5.3	1.0	1.2
Mood and Anxiety Symptom Questionnaire						
Total score	168.5	22.9	174.1	21.7	91.5	13.3
General distress anxiety subscore	23.6	5.1	25.4	6.6	12.3	1.2
General distress depression subscore	37.9	9.4	39.0	9.3	13.9	2.0
Anxious arousal subscore	24.0	6.0	25.6	6.4	18.4	2.0
Anhedonic depression subscore	82.9	11.2	84.1	9.1	47.0	11.3
Snaith-Hamilton Pleasure Scale	31.7	4.7	31.4	7.0	22.8	6.7
Duration of Current Major Depressive Episode, Months	17.3	20.0	17.6	31.9	N/A	N/A
Number of Past Depressive Episodes	3.2	2.6	3.3	3.2	N/A	N/A
	n	%	*n*	%	*n*	%
Female	28	90.3	19	73.1	22	81.5
Caucasian	20	64.5	13	50.0	13	48.1
Current Comorbid Anxiety Disorders	10	32.3	11	42.3	N/A	N/A
Past Comorbid Anxiety Disorders	13	41.9	12	46.2	N/A	N/A

Groups were matched for age, gender, race, and years of education (one-way analysis of variance; χ^2 test). All participants were right-handed. Between the major depressive disorder (MDD) groups administered amisulpride ($MDD_{Amisulpride}$) and placebo ($MDD_{Placebo}$), participants were matched for current and past comorbid anxiety disorders, as well as clinical scale measures (χ^2 test; two-sample *t* test).

HC, healthy control subjects; N/A, not applicable.

Structured Clinical Interview for DSM-IV-TR Axis I Disorders (2) was required, and exclusion criteria included psychotropic medication in the past 2 weeks (6 weeks for fluoxetine, 6 months for dopaminergic drugs or antipsychotics) and any other Axis I disorders (however, social anxiety disorder, simple phobia, or generalized anxiety disorder were allowed if secondary to MDD). For HCs, exclusion criteria were any medication in the last 3 weeks, current or past psychiatric illnesses (Structured Clinical Interview for DSM-IV-TR Axis I Disorders), and first-degree familial psychiatric illness. Participants received $15/hour in addition to earnings in the fMRI task. The two protocols were approved by Partners Human Research Committee, and all participants provided written informed consent.

Procedure

The two studies followed identical procedures, pharmacological challenge, and MRI acquisition. In the first session, a Ph.D.- or master's-level clinician administered the Structured Clinical Interview for DSM-IV-TR Axis I Disorders to determine eligibility, and participants filled out self-report scales (Table 1) (Supplement). In the second session, participants performed the MID task during fMRI scanning after receiving a single dose of amisulpride or placebo. The MID task was started 1 hour after pill administration based on pharmacokinetic data indicating that plasma concentration of amisulpride has a first peak approximately 1 to 1.5 hours after administration (17).

fMRI Task

The MID has been described in detail (10,23). Briefly, the task includes anticipation and receipt of monetary rewards (and penalties), which robustly recruit mesocorticolimbic regions (12,13) and have been used to uncover reward-related abnormalities in both magnitude of activation and functional connectivity in MDD (7,9,10,22,24).

Data Acquisition and Preprocessing

For both studies, MRI data were acquired at the McLean Imaging Center using a Siemens Tim Trio 3T MR scanner equipped with a 32-channel head coil (Siemens Medical Solutions USA, Inc., Malvern, PA). Data collection for the two studies overlapped in time. See Supplemental Methods for acquisition parameters and preprocessing.

Feature Extraction

The features used in our classifiers consisted of coefficients from the single-subject-level general linear models averaged according to the Automated Anatomical Labeling template (25). To obtain these features, for each participant, we first fitted a general linear model to the fMRI data during the MID task [see (10) for more details]. Next, for each regressor in the general linear models, the estimated coefficients were averaged according to the Automated Anatomical Labeling template, producing one averaged coefficient for each ROI. ROIs for the left and right nucleus accumbens (NAcc) were further extracted according to a manually segmented MNI-152 brain (26) and added to the existing Automated Anatomical Labeling ROIs, resulting in 118 ROIs. The following BOLD contrasts were included as features in our classification models to represent reward anticipation and consumption, respectively: 1) reward cue minus neutral cue and 2) reward outcome minus

no-change outcome following reward cue. In addition, two striatal connectivity features emerging from our previous work (10) were included in our classification models, representing the psychophysiological interaction under the reward outcome condition between 1) caudate and dorsal ACC and 2) NAcc and midcingulate cortex (MCC). In total, 238 features (118 ROIs $\times$ 2 contrasts + 2 psychophysiological interactions) were included in the classification models. Modeling was also done without the psychophysiological interaction regressors to establish if they brought any additional predictive information (see Supplement). All features were standardized to zero mean and unit variance before being entered into the models.

Classification and Importance-Guided Sequential Model Selection

Two main classifiers were built to classify 1) $MDD_{Placebo}$ versus $HC_{Placebo}$ and 2) $MDD_{Placebo}$ versus $MDD_{Amisulpride}$. These were designed to capture features linked to 1) MDD and 2) the effect of short-term dopaminergic enhancement on whole-brain BOLD activation in individuals with MDD. To further test the hypothesis that dopaminergic enhancement transiently normalized reward-related abnormalities in MDD, a third classifier was built to classify $MDD_{Amisulpride}$ versus $HC_{Placebo}$. Across analyses, we used logistic regression with elastic net regularization (27) for classification. The elastic net regularization is well suited for problems where the number of features is much greater than the number of observations (27). The models were trained and tested via the following nested cross-validation procedure. First, we performed model training on a development set containing 80% of the participants via a threefold grid search cross-validation procedure (stratified using class labels) (Figure 1B). Then, the model with the best regularization parameters was further tested on the evaluation set containing an independent set of 20% participants, which the model had not seen during the training and validation phases. The above procedure was repeated 100 times to ensure that stable performance was obtained on a large number of development-evaluation splits. The area under the receiver operating characteristics curve (AUC) was selected as the metric to quantify model performance, and reported AUCs are only from testing on the independent evaluation set.

To identify the set of most predictive features for each classifier (i.e., $MDD_{Placebo}$ vs. $HC_{Placebo}$ and $MDD_{Placebo}$ vs. $MDD_{Amisulpride}$), we adopted the following importance-guided sequential model selection procedure (Figure 1A). Specifically, we first rank-ordered the features using the mean model weights across 100 implementations as a measure of predictability. Then, we built a series of truncated models such that each model only took the top k most predictive features as inputs to perform the classification tasks, with k varying from the top 1 most predictive feature to the number of participants involved in a given classifier. Imposing the number of participants as the upper limit was to ensure that models' performance was not mainly driven by the regularization term. All truncated models underwent the nested cross-validation procedure described above, and the test performance from each truncated model on the independent evaluation set was obtained. The set of features used by the truncated model achieving the highest AUC on the evaluation set was deemed as the optimal feature set.

After identifying the best truncated models for the classifiers, we compared the feature sets—both the selected regions and the regression weight signs (positive or negative), as they indicated the direction of the BOLD difference (greater for one class over another). Based on how we set up the classifiers, those regions shared by the $MDD_{Placebo}$ versus $HC_{Placebo}$ and $MDD_{Placebo}$ versus $MDD_{Amisulpride}$ classifiers with convergent regression signs constitute a potential multivariate signature that we can use to assess amisulpride-induced BOLD normalization in MDD subjects. We calculated signed BOLD sum scores by summing up the BOLD values of the convergent features multiplied by the regression weight sign to assess normalization. The convergent features should largely be absent in the set of highly differentiating features of the $MDD_{Amisulpride}$ versus $HC_{Placebo}$ classifier if they have been normalized with amisulpride.

Statistical Analysis

The significance of the models' performances against chance level was tested using a random permutation test scheme in which the truncated model based on the optimal feature set were retrained on label shuffled training data (28). The entire test procedure was iterated 1000 times to empirically construct the null distribution of test AUCs. The p values were obtained by comparing the AUC from the best truncated model based on unshuffled data against the empirical null distribution. The performances between models were statistically compared via Mann-Whitney U tests. Effect sizes between two distributions were calculated using Cohen's d.

RESULTS

Classification Performances

The best truncated models selected by the importance-guided model selection procedure (Figure 1) based on most predictive features from whole-brain BOLD activations and striatal connectivity achieved high predictive performances (Table 2) (see Supplemental Figure S1 for model performance as a function of top features). For both $MDD_{Placebo}$ versus $HC_{Placebo}$ and $MDD_{Placebo}$ versus $MDD_{Amisulpride}$, the AUCs of the best truncated models were significantly above chance level ($MDD_{Placebo}$ vs. $HC_{Placebo}$: mean AUC = 0.87, permutation testing $p = .004$; $MDD_{Placebo}$ vs. $MDD_{Amisulpride}$: mean AUC = 0.89, $p = .002$) (Figure 2A, B) (Supplemental Figure S2). Predictive features displayed some collinearity, but collinearity did not account for the diminishing AUC returns of the lower-ranked predictive features (see Supplemental Results and Supplemental Figures S3 and S4). Compared with models trained using striatal features only (Supplemental Methods), the performances of the best truncated models based on whole-brain features were significantly better for both contrasts (both $p < .001$, Mann-Whitney U test). The histograms of sum scores created by summing up the top feature values while taking into account the sign of the corresponding model weights demonstrated high separability between $MDD_{Placebo}$ and $HC_{Placebo}$ as well as between $MDD_{Placebo}$ and $MDD_{Amisulpride}$ (Figure 2C, D). Overall, these results indicate that our models were able to extract highly predictive information embedded in the whole-brain BOLD signal.

Table 2. Classification Performance for the Best Truncated Models

	$MDD_{Placebo}$ vs. $HC_{Placebo}$		$MDD_{Placebo}$ vs. $MDD_{Amisulpride}$		Striatum Only: $MDD_{Placebo}$ vs. $HC_{Placebo}$		Striatum Only: $MDD_{Placebo}$ vs. $MDD_{Amisulpride}$	
	Mean	SD	Mean	SD	Mean	SD	Mean	SD
AUC	0.87	0.12	0.89	0.09	0.59	0.14	0.61	0.17
Accuracy	0.77	0.12	0.80	0.10	0.59	0.13	0.59	0.13
Sensitivity	0.84	0.18	0.89	0.11	0.58	0.25	0.65	0.19
Specificity	0.72	0.22	0.67	0.24	0.59	0.22	0.50	0.28
Number of Features	48		44		6		11	

AUC, area under the curve; HC, healthy control subjects; MDD, major depressive disorder.

Brain Regions Specific to Reward Anticipation

Positive Model Weights. The best truncated model for $MDD_{Placebo}$ versus $MDD_{Amisulpride}$ identified the lateral orbitofrontal cortex (lOFC), visual cortex, ACC, dorsomedial prefrontal cortex, MCC, and precuneus as most predictive features with positive weights during reward anticipation (Figure 3A and Supplemental Table S1). This indicates that within the MDD group, BOLD activation in these regions related to the contrast of reward cue minus neutral cue was reduced following administration of amisulpride compared with placebo. Critically, the lOFC, visual cortex, and MCC were also selected by the best $MDD_{Placebo}$ versus $HC_{Placebo}$ model as top features having positive weights (Figure 3B and Supplemental Table S2), and at the same time these regions, except a right occipital region, were not among the most predictive features in the $MDD_{Amisulpride}$ versus $HC_{Placebo}$ model (Supplemental Figure S5). Collectively, these findings indicate that within the MDD group, amisulpride largely normalized the heightened BOLD activation in these regions toward reward cues. Other regions with positive weights in the $MDD_{Placebo}$ versus $HC_{Placebo}$ classification included the thalamus, supplementary motor area, and ventromedial prefrontal cortex. Again, these regions were not among the top features in the $MDD_{Amisulpride}$ versus $HC_{Placebo}$ model (Supplemental Figure S5), suggesting that amisulpride mitigated the hyperactivation in these regions within the MDD group.

Negative Model Weights. Regions selected by the best $MDD_{Placebo}$ versus $MDD_{Amisulpride}$ model with negative model weights included the putamen, pallidum, amygdala, posterior parietal cortex (PPC), and temporal cortex (Figure 3A and Supplemental Table S1). The negative weights observed in the putamen and pallidum were consistent with the hypothesis that amisulpride might have increased dopaminergic signaling in the basal ganglia in MDD (10,14). This effect is rather pronounced as the $MDD_{Amisulpride}$ versus $HC_{Placebo}$ model showed that the contrast of reward cue minus neutral cue evoked higher activation in the putamen in the $MDD_{Amisulpride}$ group even compared with the $HC_{Placebo}$ group (Supplemental Figure S5). Within the $MDD_{Placebo}$ group, reduced activation

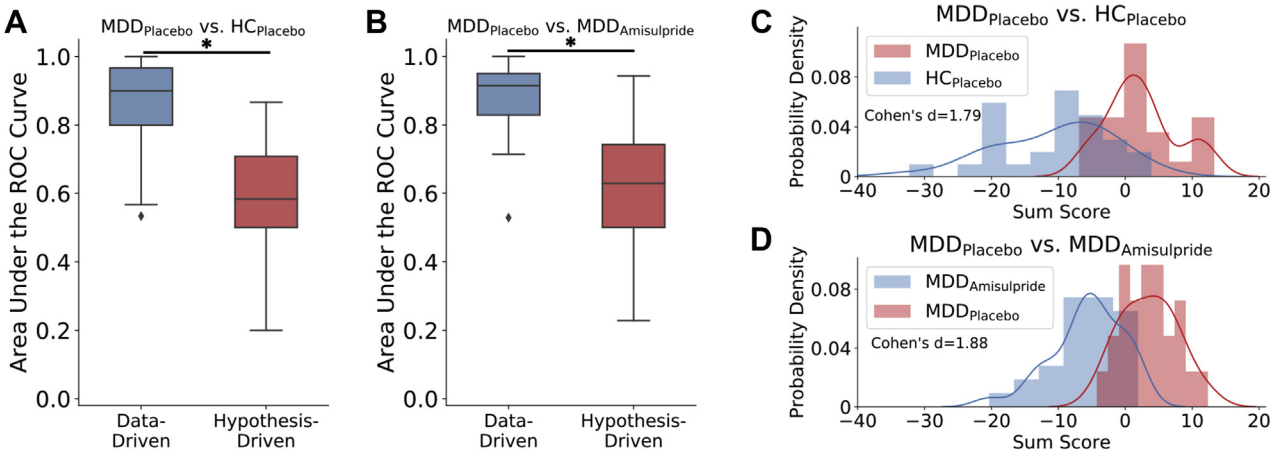

Figure 2. Comparing classification performance between the data-driven models based on features selected from the whole-brain and the hypothesis-driven models based only on striatal features for **(A)** $MDD_{Placebo}$ vs. $HC_{Placebo}$ and **(B)** $MDD_{Placebo}$ vs. $MDD_{Amisulpride}$ classifications. Asterisks denote significantly different median area under the receiver operating characteristic (ROC) curve measures between the data-driven and hypothesis-driven models as assessed by the Mann-Whitney *U* test. The black markers denote outliers falling outside the ±1.5 interquartile range. The histogram of the signed sum score from the model-identified most predictive brain regions show high separability between **(C)** $MDD_{Placebo}$ vs. $HC_{Placebo}$ and **(D)** $MDD_{Placebo}$ vs. $MDD_{Amisulpride}$. HC, healthy control subjects; MDD, major depressive disorder.

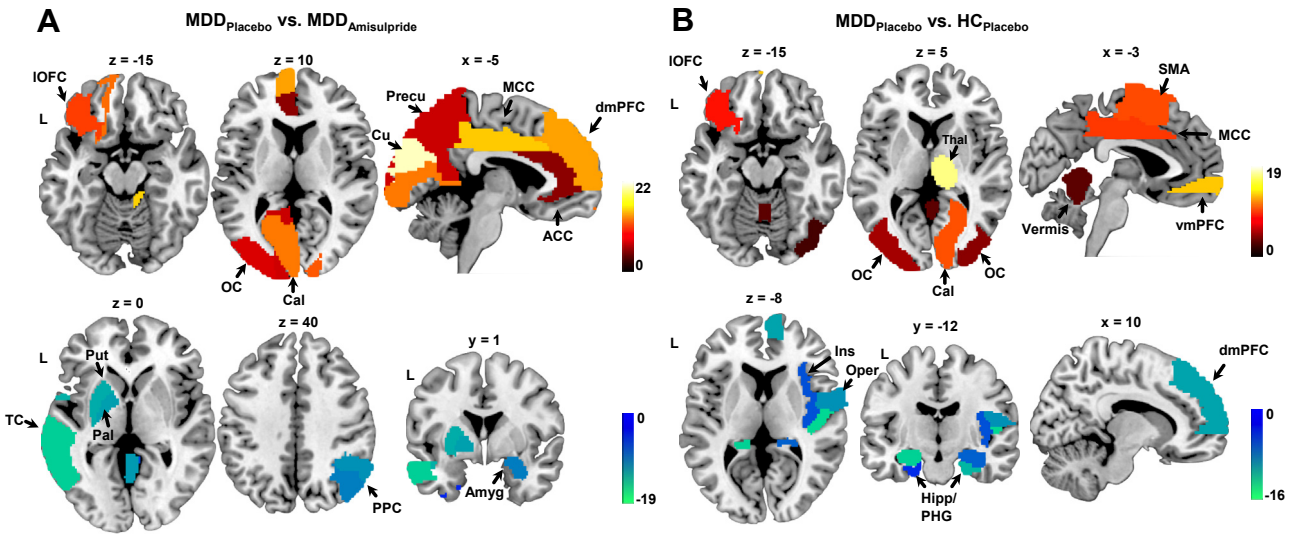

Figure 3. Weight maps showing the most predictive brain regions for the contrast of the reward minus neutral cue conditions. **(A)** Weight map for the $MDD_{Placebo}$ vs. $MDD_{Amisulpride}$ model. Positive weights indicate higher blood oxygen level–dependent values in the $MDD_{Placebo}$ group relative to the $MDD_{Amisulpride}$ group and negative weights indicate the opposite direction. **(B)** Weight map for the $MDD_{Placebo}$ vs. $HC_{Placebo}$ model, with positive weights indicating higher blood oxygen level–dependent values in the $MDD_{Placebo}$ group relative to the $HC_{Placebo}$ group and vice versa. ACC, anterior cingulate cortex; Amyg, amygdala; Cal, calcarine sulcus; Cu, cuneus; dmPFC, dorsomedial prefrontal cortex; HC, healthy control subjects; Hipp, hippocampus; Ins, insula; L, left; lOFC, lateral orbitofrontal cortex; MCC, midcingulate cortex; MDD, major depressive disorder; OC, occipital cortex; Oper, operculum; Pal, pallidum; PHG, parahippocampal gyrus; PPC, posterior parietal cortex; Precu, precuneus; Put, putamen; SMA, supplementary motor area; TC, temporal cortex; Thal, thalamus; vmPFC, ventromedial prefrontal cortex.

in the operculum, hippocampus, parahippocampal gyrus (PHG), and dorsomedial prefrontal cortex was observed relative to HCs during reward anticipation (features in the $MDD_{Placebo}$ vs. $HC_{Placebo}$ model with negative weights) (Figure 3B and Supplemental Table S2). The reduced activation in the hippocampus and operculum persisted in the $MDD_{Amisulpride}$ versus $HC_{Placebo}$ model (Supplemental Figure S5), indicating that amisulpride had limited effects in these regions.

Brain Regions Specific to Reward Consumption

Positive Model Weights. Examining features selected from the contrast of reward minus no change outcomes in the $MDD_{Placebo}$ versus $MDD_{Amisulpride}$ model revealed that the lOFC, posterior parietal cortex (PPC), superior frontal gyrus, and the pre- and postcentral gyrus were selected as most predictive features with positive weights (Figure 4A and Supplemental Table S3). This indicates reduced activation in these regions during reward consumption in $MDD_{Amisulpride}$ compared with $MDD_{Placebo}$. Of note, the lOFC and PPC emerged as among the most predictive features with positive weights in the $MDD_{Placebo}$ versus $HC_{Placebo}$ model (Figure 4C and Supplemental Table S4). Additionally, while the lOFC hyperactivation was still observed in the $MDD_{Amisulpride}$ versus $HC_{Placebo}$ model, the PPC was not identified as a predictive feature (Supplemental Figure S5). Overall, these results suggest that under placebo, the MDD group was characterized by increased BOLD activity in these regions during reward consumption relative to HCs and that the hyperactivation was reduced by amisulpride. Other brain regions identified as most predictive features with positive weights in the $MDD_{Placebo}$ versus $HC_{Placebo}$ model included the inferior frontal gyrus, PPC, precuneus, and MCC. The lack of predictability from these regions between $MDD_{Amisulpride}$ and $HC_{Placebo}$ (Supplemental Figure S5) again suggests a mitigating effect of amisulpride on the hyperactivation in these regions.

Negative Model Weights. The most predictive regions from the contrast of reward minus no-change outcomes with negative weights in the $MDD_{Placebo}$ versus $MDD_{Amisulpride}$ model included the putamen, NAcc, PHG, and temporal pole (Figure 4A and Supplemental Table S3), as well as the connectivity between the NAcc and MCC (Figure 4B). This suggests that within the MDD group, amisulpride increased BOLD activation and corticostriatal connectivity to reward feedback in these regions. Highlighting again convergence, the NAcc, PHG, temporal pole, and the NAcc-MCC connectivity were also selected as most predictive features having negative weights in the $MDD_{Placebo}$ versus $HC_{Placebo}$ classification (Figure 4C, D and Supplemental Table S4), and none of these regions was selected as among the top predictive features in the $MDD_{Amisulpride}$ versus $HC_{Placebo}$ model (Supplemental Figure S5). Thus, in MDD, amisulpride normalized both hypoactivation and hypoconnectivity in response to rewards in these regions. Other most predictive features with negative weights in the $MDD_{Placebo}$ versus $HC_{Placebo}$ model included the visual cortex, inferior temporal cortex, operculum, ACC, and the connectivity between the caudate and dorsal ACC. These features, except the caudate-dorsal ACC connectivity, were not identified as among the top features in the $MDD_{Amisulpride}$ versus $HC_{Placebo}$ model (Supplemental Figure S5), indicating increased activation to rewards in these regions following

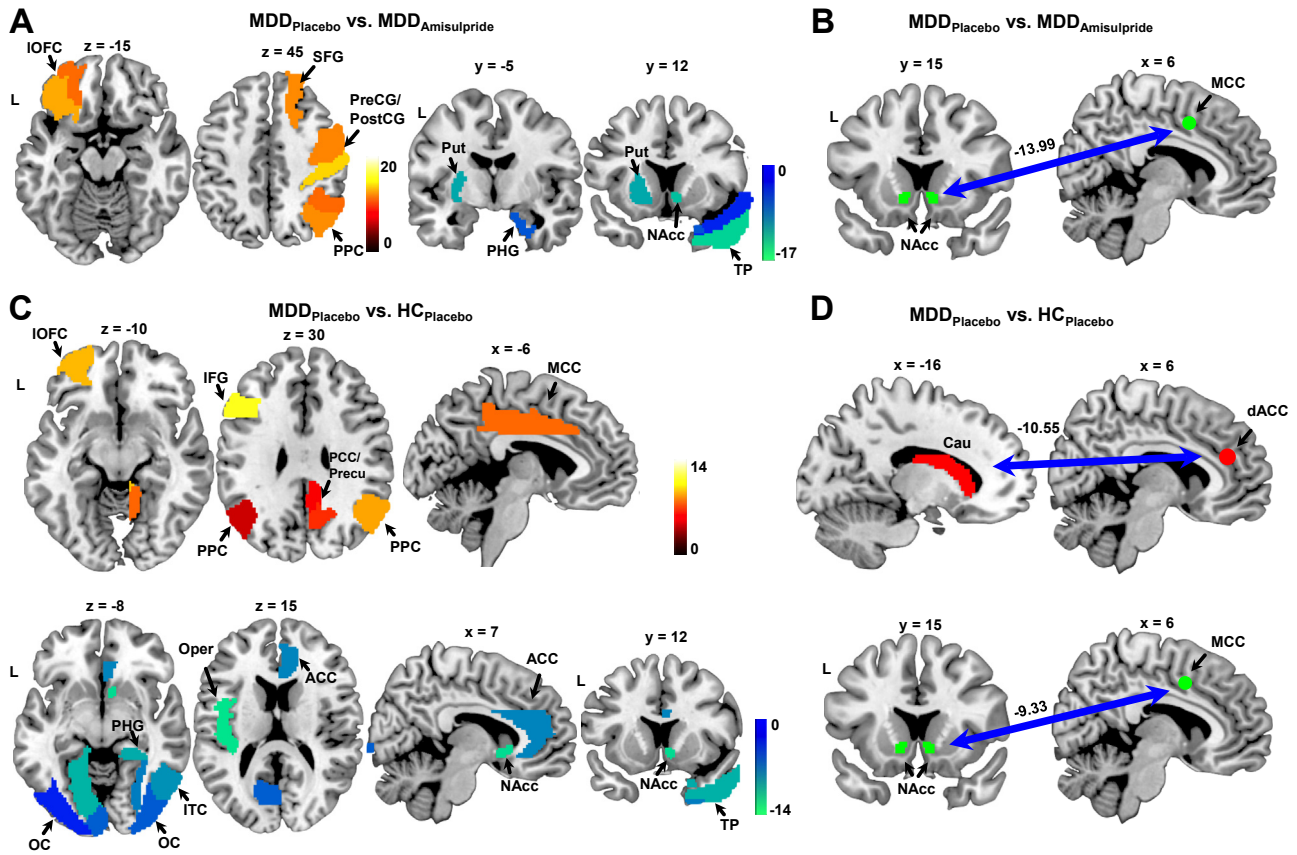

Figure 4. Weight maps showing the most predictive brain regions and/or connectivity for the contrast of reward minus no-change outcomes. **(A)** Weight map for the $MDD_{Placebo}$ vs. $MDD_{Amisulpride}$ model, with positive weights indicating higher blood oxygen level–dependent values in the $MDD_{Placebo}$ group relative to the $MDD_{Amisulpride}$ group and vice versa. **(B)** Negative weight assigned to the nucleus accumbens (NAcc)-midcingulate cortex (MCC) connectivity in the $MDD_{Placebo}$ vs. $MDD_{Amisulpride}$ model. **(C)** Weight map for the $MDD_{Placebo}$ vs. $HC_{Placebo}$ model. Positive weights indicate higher blood oxygen level–dependent values in the $MDD_{Placebo}$ group relative to the $MDD_{Amisulpride}$ group and vice versa. **(D)** Negative weights assigned to the caudate (Cau)-dorsal anterior cingulate cortex (dACC) and NAcc-MCC connectivity features by the $MDD_{Placebo}$ vs. $HC_{Placebo}$ model. CG, central gyrus; HC, healthy control subjects; IFG, inferior frontal gyrus; ITC, inferior temporal cortex; L, left; lOFC, lateral orbitofrontal cortex; MDD, major depressive disorder; OC, occipital cortex; Oper, operculum; PCC, posterior cingulate cortex; PHG, parahippocampal gyrus; PPC, posterior parietal cortex; Precu, precuneus; Put, putamen; SFG, superior frontal gyrus; TP, temporal pole.

amisulpride administration in the MDD group. The fact that amisulpride did not normalize the hypoconnectivity between caudate and dorsal ACC in the MDD group is consistent with previously published ROI-based results obtained on a subset of the participants (10).

A Multivariate Signature of Normalization

The signed BOLD sum scores calculated from the convergent features across the $MDD_{Placebo}$ versus $HC_{Placebo}$ and $MDD_{Placebo}$ versus $MDD_{Amisulpride}$ classifiers showed that the multivariate neural signature is significantly greater in the $MDD_{Placebo}$ than in either $MDD_{Amisulpride}$ or $HC_{Placebo}$ groups (Figure 5) (all $p < .001$, Mann-Whitney U test), while the latter two groups were statistically equivalent based on equivalence testing ($p = .01$) (see the Supplement for more information). Taken together, these results suggest that amisulpride normalized MDD-related abnormalities.

DISCUSSION

This study used a machine learning–based approach to identify reliable brain-wide features that delineated MDD-related abnormalities as well as features linked to their normalization after an acute dopaminergic pharmacological challenge. In addition to increased striatal activation in the $MDD_{Amisulpride}$ relative to $MDD_{Placebo}$ group [which is consistent with ROI-based conventional analyses of a smaller subset of the participants included here (10)], the classification model also identified an extensive set of reward-related brain regions differentiating these groups, which provided additional predictive power over striatal regions alone. Converging of features between the $MDD_{Placebo}$ versus $MDD_{Amisulpride}$ model and the $MDD_{Placebo}$ versus $HC_{Placebo}$ model suggested that amisulpride had a bidirectionally normalizing effect on reward-related activation and functional connectivity of brain regions

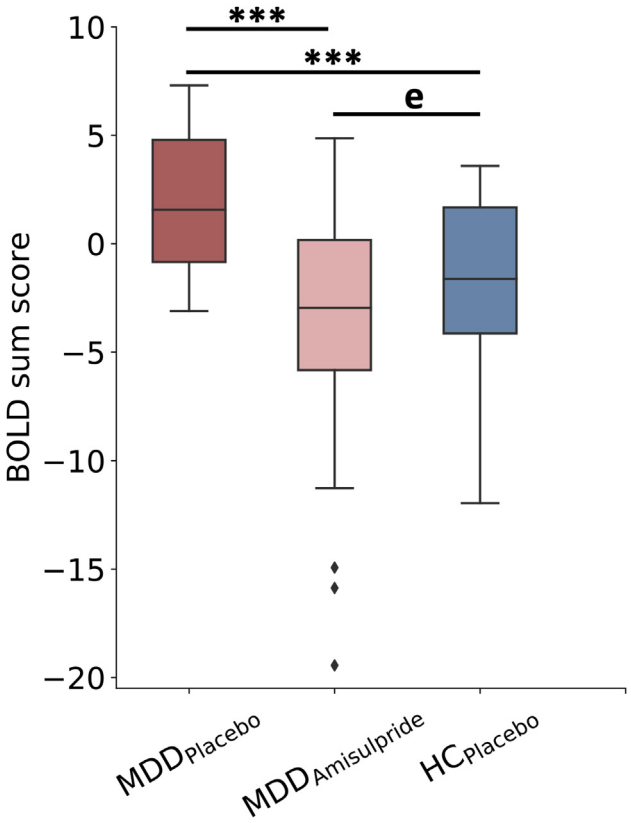

Figure 5. Multivariate signatures across groups demonstrated amisulpride-based brain normalization. The signed blood oxygen level–dependent (BOLD) sum scores calculated across the convergent features of $MDD_{Placebo}$ vs. $MDD_{Amisulpride}$ and $MDD_{Placebo}$ vs. $HC_{Placebo}$ models suggest normalization of MDD-related abnormalities following amisulpride administration. $MDD_{Placebo}$ subjects had overall greater multivariate neural signatures compared to $HC_{Placebo}$ or $MDD_{Amisulpride}$ (***$p < .001$ for both tests). Equivalence testing demonstrated that $HC_{Placebo}$ and $MDD_{Amisulpride}$ had statistically equivalent (denoted using "e" in plot) scores ($p = .01$). HC, healthy control subjects; MDD, major depressive disorder.

spanning the lOFC, NAcc, PHG, MCC, PPC, and areas of the visual cortex among depressed individuals. Taken together, these results highlight the unique contribution of machine learning–based approaches to examine brain-wide circuit engagement and potential normalization after a single dose. Such mechanistic evidence can help evaluate novel compounds before pursuing longer efficacy-oriented clinical trials with a compound. Overall, this study provided novel evidence for the mechanism through which (transient) dopaminergic enhancement might restore system-level activity during reward processing among individuals with MDD.

Amisulpride appeared to have bidirectional normalizing effects on brain activation and functional coordination among depressed individuals. Within the striatum, consistent with previous ROI-based analyses based on a subset of the participants used here (10), results from our classification models showed that while striatal–basal ganglia activation and corticostriatal connectivity were initially decreased among depressed individuals, they were enhanced following acute administration of amisulpride [see (29) for conceptually similar imaging findings using a single dose of the novel D_2 antagonist lurasidone]. This supports the validity of the importance-guided model selection procedure and fits the view that lower doses of amisulpride enhance dopaminergic signaling in the striatum (17).

Among regions outside the striatum, one notable finding was that increased lOFC activation during reward anticipation in MDD was reduced after administration of amisulpride. Neurophysiological evidence has shown that subpopulations of neurons in the lOFC respond to nonreward or unpleasant events and maintain elevated firing rate after such events (30). This led to the theory implicating overly reactive and prolonged activation of the lOFC nonreward circuit as a potential mechanism underlying depression (31). Previous studies have documented increased lOFC activation in MDD (32), and our result fits this theoretical view. In the $MDD_{Amisulpride}$ group, reduced lOFC activation suggests that amisulpride may normalize reward processing by decreasing lOFC hyperactivation, consistent with previous reports that improvements in depressive symptoms were accompanied by reduced lOFC activation (33) and that electrical stimulation of the lOFC acutely improved depressive symptoms (34).

In addition to effects in frontostriatal circuitry, amisulpride restored hypoactivation in the PHG and temporal pole in MDD. The hippocampus and parahippocampal complex connect with the medial OFC and are hypothesized to facilitate the formation of episodic memory regarding reward (35). Decreased hippocampal activation has emerged in MDD, and prolonged or repeated depressive episodes have been linked to reduced hippocampal volume (36,37). These abnormalities have been linked to dysfunctions in both memory encoding and retrieval characteristic of MDD, even after treatment (38,39). The fact that amisulpride restored parahippocampal and temporal pole activation suggests that interventions aiming to increase dopaminergic signaling might improve encoding and retrieval of positive memories in MDD. However, it should be noted that hippocampal activation did not differentiate between the $MDD_{Amisulpride}$ and $MDD_{Placebo}$ groups, suggesting that the effects on memory might be limited following a single acute pharmacological challenge.

Hyperactivation in the MCC toward the reward cue was also reduced among depressed individuals after amisulpride. Moreover, amisulpride also reduced reward cue-evoked activations in adjacent ACC and dorsomedial prefrontal cortex. The supracallosal part of the cingulate cortex receives neuronal projections from the lOFC and is thought to also encode nonreward and punishing events such as physical and social pain (40,41). A recent study has identified a nociceptive pathway between the MCC and posterior insula responsible for generating a hypersensitive state for pain, providing a mechanism for the increased pain sensitivity by psychosocial factors (42). The reduced hyperactivation in these regions following amisulpride administration may indicate decreased sensitivity to negative affective states among individuals with MDD and therefore priming or biasing them toward reward.

In MDD, amygdalar activation evoked by reward cues was enhanced following administration of amisulpride. Reduced amygdalar response to positive and rewarding stimulus, coupled with heightened amygdalar activation toward

negative stimulus, are well-documented findings in MDD, which highlights an imbalanced reactivity toward emotionally salient cues (43). Antidepressant treatment has been shown to address this imbalance by partially normalizing the bidirectional abnormal amygdalar activation (43,44). These findings were further bolstered by the recent report that enhanced amygdalar response toward positive memories through real-time fMRI neurofeedback was associated with reduction in depressive symptoms (45). The increased amygdalar activation evoked by reward cues is consistent with these studies and implicates improved sensitivity toward reward following acute dopaminergic enhancement.

While several regions showed predictive power following the administration of amisulpride, it is difficult to assess whether changes in these regions reflected a direct modulation resulting from the enhanced dopaminergic signaling or alternatively reflected secondary responses through network interactions. Future studies could utilize network analysis and/or neural perturbation methods to further dissociate direct versus indirect effects (34). In addition, amisulpride also has 5-HT_7 (5-hydroxytryptamine receptor 7) antagonism (46), which has been hypothesized to contribute to its antidepressant property. While we cannot rule out that the effects observed here may be partially caused by this off-target mechanism, additional research is needed to distinguish the effect of dopaminergic enhancement versus 5-HT_7 antagonism of amisulpride. Lastly, we only focused on investigating the effects of dopaminergic enhancement on reward processing among depressed individuals. Future studies could seek to examine the effect of enhanced dopamine on whole-brain fMRI activity in depression under additional conditions; additionally, based on hypotheses of shared mesocorticolimbic dopaminergic abnormalities, this molecule could be tested in other disorders such as addiction or schizophrenia [e.g., (47,48)].

ACKNOWLEDGMENTS AND DISCLOSURES

This project was supported by the National Institute of Mental Health (Grants Nos. R01 MH068376, R37 MH068376, and R01MH095809 [to DAP]). The content is solely the responsibility of the authors and does not necessarily represent the official views of the National Institutes of Health.

DAP designed both studies and obtained funding for both; RC, MB, FG, and GV collected data; YL, MM, RA, ELB, RHK performed the analyses; YL, DAP, RA, MM, and PA wrote the manuscript. All authors approved the manuscript.

Data are available at the NIMH Data Archive (https://nda.nih.gov/).

Analysis scripts are available upon request.

YL, MM, and PA are current or previous full-time employees at Blackthorn Therapeutics Inc. Over the past 3 years, DAP has received consulting fees from Akili Interactive Labs, BlackThorn Therapeutics, Boehringer Ingelheim, Posit Science, and Takeda Pharmaceuticals and an honorarium from Alkermes for activities unrelated to the current review. All other authors report no biomedical financial interests or potential conflicts of interest.

ClinicalTrials.gov: The Effects of Dopamine on Reward Processing; http:// https://clinicaltrials.gov/ct2/show/NCT01253421; NCT01253421; and An Investigation of Early Life Stress and Depression; http:// https://clinicaltrials.gov/ct2/show/NCT01701258; NCT01701258.

ARTICLE INFORMATION

From the BlackThorn Therapeutics (YL, MSM, PA), San Francisco, California; Department of Psychology (RA), University of Haifa, Haifa, Israel; McLean Hospital (ELB, RC, MB, FG, GV, DAP), Belmont, Massachusetts; Department of Psychiatry (ELB, GV, DAP), Harvard Medical School, Boston, Massachusetts; and Department of Psychology and Neuroscience (RHK), University of Colorado, Boulder, Colorado.

PA and DAP contributed equally to this work.

Address correspondence to Diego A. Pizzagalli, Ph.D., Center for Depression, Anxiety and Stress Research, McLean Hospital, 115 Mill Street, Belmont, MA 02478; E-mail: dap@mclean.harvard.edu.

Received Sep 3, 2019; revised Sep 30, 2019; accepted Oct 1, 2019.

Supplementary material cited in this article is available online at https://doi.org/10.1016/j.bpsc.2019.10.002.

REFERENCES

1. Calabrese JR, Fava M, Garibaldi G, Grunze H, Krystal AD, Laughren T, *et al.* (2014): Methodological approaches and magnitude of the clinical unmet need associated with amotivation in mood disorders. J Affect Disorders 168:439–451.
2. American Psychiatric Association (2000): Diagnostic and Statistical Manual of Mental Disorders, 4th ed, Text Revision: DSM-IV-TR. Washington, DC: American Psychiatric Publishing.
3. Wise RA (2004): Dopamine, learning and motivation. Nat Rev Neurosci 5:483–494.
4. Berridge KC, Kringelbach ML (2015): Pleasure systems in the brain. Neuron 86:646–664.
5. Der-Avakian A, Markou A (2012): The neurobiology of anhedonia and other reward-related deficits. Trends Neurosci 35:68–77.
6. Husain M, Roiser JP (2018): Neuroscience of apathy and anhedonia: A transdiagnostic approach. Nat Rev Neurosci 19:470–484.
7. Pizzagalli DA, Holmes AJ, Dillon DG, Goetz EL, Birk JL, Bogdan R, *et al.* (2009): Reduced caudate and nucleus accumbens response to rewards in unmedicated individuals with major depressive disorder. Am J Psychiatry 166:702–710.
8. Pizzagalli DA (2014): Depression, stress, and anhedonia: Toward a synthesis and integrated model. Annu Rev Clin Psychol 10:393–423.
9. Admon R, Nickerson LD, Dillon DG, Holmes AJ, Bogdan R, Kumar P, *et al.* (2014): Dissociable cortico-striatal connectivity abnormalities in major depression in response to monetary gains and penalties. Psychol Med 45:121–131.
10. Admon R, Kaiser RH, Dillon DG, Beltzer M, Goer F, Olson DP, *et al.* (2017): Dopaminergic enhancement of striatal response to reward in major depression. Am J Psychiatry 174:378–386.
11. McClure SM, York MK, Montague RP (2004): The neural substrates of reward processing in humans: the modern role of fMRI. Neuroscientist 10:260–268.
12. Oldham S, Murawski C, Fornito A, Youssef G, Yücel M, Lorenzetti V (2018): The anticipation and outcome phases of reward and loss processing: A neuroimaging meta-analysis of the monetary incentive delay task. Hum Brain Mapp 39:3398–3418.
13. Wilson RP, Colizzi M, Bossong MG, Allen P, Kempton M, MTAC, *et al.* (2018): The neural substrate of reward anticipation in health: A meta-analysis of fMRI findings in the monetary incentive delay task. Neuropsychol Rev 28:496–506.
14. Schott BH, Minuzzi L, Krebs RM, Elmenhorst D, Lang M, Winz OH, *et al.* (2008): Mesolimbic functional magnetic resonance imaging activations during reward anticipation correlate with reward-related ventral striatal dopamine release. J Neurosci 28:14311–14319.
15. Amore M, Jori M (2001): Faster response on amisulpride 50 mg versus sertraline 50-100 mg in patients with dysthymia or double depression: A randomized, double-blind, parallel group study. Int Clin Psychopharmacol 16:317–324.
16. Cassano G, Jori M (2002): Efficacy and safety of amisulpride 50 mg versus paroxetine 20 mg in major depression: A randomized, double-blind, parallel group study. Int Clin Psychopharmacol 17:27–32.
17. Rosenzweig P, Canal M, Patat A, Bergougnan L, Zieleniuk I, Bianchetti G (2002): A review of the pharmacokinetics, tolerability and pharmacodynamics of amisulpride in healthy volunteers. Hum Psychopharmacol 17:1–13.

18. Viviani R, Graf H, Wiegers M, Abler B (2013): Effects of amisulpride on human resting cerebral perfusion. Psychopharmacology (Berl) 229:95–103.
19. Metzger CD, Wiegers M, Walter M, Abler B, Graf H (2016): Local and global resting state activity in the noradrenergic and dopaminergic pathway modulated by reboxetine and amisulpride in healthy subjects. Int J Neuropsychoph 19:1–9.
20. Forbes EE, Hariri AR, Martin SL, Silk JS, Moyles DL, Fisher PM, *et al.* (2009): Altered striatal activation predicting real-world positive affect in adolescent major depressive disorder. Am J Psychiatry 166:64–73.
21. Kumar P, Waiter G, Ahearn T, Milders M, Reid I, Steele JD (2008): Abnormal temporal difference reward-learning signals in major depression. Brain 131:2084–2093.
22. Stoy M, Schlagenhauf F, Sterzer P, Bermpohl F, Hägele C, Suchotzki K, *et al.* (2012): Hyporeactivity of ventral striatum towards incentive stimuli in unmedicated depressed patients normalizes after treatment with escitalopram. J Psychopharmacol 26:677–688.
23. Knutson B, Westdorp A, Kaiser E, Hommer D (2000): FMRI visualization of brain activity during a monetary incentive delay task. Neuroimage 12:20–27.
24. Knutson B, Bhanji JP, Cooney RE, Atlas LY, Gotlib IH (2008): Neural responses to monetary incentives in major depression. Biol Psychiatry 63:686–692.
25. Tzourio-Mazoyer N, Landeau B, Papathanassiou D, Crivello F, Etard O, Delcroix N, *et al.* (2002): Automated anatomical labeling of activations in SPM using a macroscopic anatomical parcellation of the MNI MRI single-subject brain. Neuroimage 15:273–289.
26. Admon R, Holsen LM, Aizley H, Remington A, Whitfield-Gabrieli S, Goldstein JM, *et al.* (2015): Striatal hypersensitivity during stress in remitted individuals with recurrent depression. Biol Psychiatry 78:67–76.
27. Zou H, Hastie T (2005): Regularization and variable selection via the elastic net. J R Stat Soc Series B Stat Methodol 67:301–320.
28. Ojala M, Garriga GC (2010): Permutation tests for studying classifier performance. J Mach Learn Res 11:1833–1863.
29. Wolke SA, Mehta MA, O'Daly O, Zelaya F, Zahreddine N, Keren H, *et al.* (2019): Modulation of anterior cingulate cortex reward and penalty signalling in medication-naive young-adult subjects with depressive symptoms following acute dose lurasidone. Psychol Med 49:1365–1377.
30. Thorpe S, Rolls ET, Maddison S (1983): The orbitofrontal cortex: neuronal activity in the behaving monkey. Exp Brain Res 49:93–115.
31. Rolls ET (2016): A non-reward attractor theory of depression. Neurosci Biobehav Rev 68:47–58.
32. Cheng W, Rolls ET, Qiu J, Liu W, Tang Y, Huang C, *et al.* (2016): Medial reward and lateral non-reward orbitofrontal cortex circuits change in opposite directions in depression. Brain 139:3296–3309.
33. Brody AL, Saxena S, Mandelkern MA, Fairbanks LA, Ho ML, Baxter LR (2001): Brain metabolic changes associated with symptom factor improvement in major depressive disorder. Biol Psychiatry 50:171–178.
34. Rao VR, Sellers KK, Wallace DL, Lee MB, Bijanzadeh M, Sani OG, *et al.* (2018): Direct electrical stimulation of lateral orbitofrontal cortex acutely improves mood in individuals with symptoms of depression. Curr Biol 28:3893–3902.
35. Suzuki WA, Naya Y (2014): The perirhinal cortex. Annu Rev Neurosci 37:39–53.
36. Milne A, MacQueen GM, Hall GBC (2012): Abnormal hippocampal activation in patients with extensive history of major depression: an fMRI study. J Psychiatry Neurosci 37:28–36.
37. McKinnon MC, Yucel K, Nazarov A, MacQueen GM (2009): A meta-analysis examining clinical predictors of hippocampal volume in patients with major depressive disorder. J Psychiatry Neurosci 34:41–54.
38. Dillon DG (2015): The neuroscience of positive memory deficits in depression. Front Psychol 6:1295.
39. Dillon DG, Pizzagalli DA (2018): Mechanisms of memory disruption in depression. Trends Neurosci 41:137–149.
40. Grabenhorst F, Rolls ET (2011): Value, pleasure and choice in the ventral prefrontal cortex. Trends Cogn Sci 15:56–67.
41. Rotge JY, Lemogne C, Hinfray S, Huguet P, Grynszpan O, Tartour E, *et al.* (2015): A meta-analysis of the anterior cingulate contribution to social pain. Soc Cogn Affect Neursci 10:19–27.
42. Tan L, Pelzer P, Heinl C, Tang W, Gangadharan V, Flor H, *et al.* (2017): A pathway from midcingulate cortex to posterior insula gates nociceptive hypersensitivity. Nat Neurosci 20:1591–1601.
43. Victor TA, Furey ML, Fromm SJ, Öhman A, Drevets WC (2010): Relationship between amygdala responses to masked faces and mood state and treatment in major depressive disorder. Arch Gen Psychiatry 67:1128–1138.
44. Fu CH, Williams SCR, Cleare AJ, Brammer MF, Walsh ND, Kim J, *et al.* (2004): Attenuation of the neural response to sad faces in major depression by antidepressant treatment: a prospective, event-related functional magnetic resonance imaging study. Arch Gen Psychiatry 61:877–889.
45. Young KD, Siegle GJ, Zotev V, Phillips R, Misaki M, Yuan H, *et al.* (2017): Randomized clinical trial of real-time fMRI amygdala neurofeedback for major depressive disorder: Effects on symptoms and autobiographical memory recall. Am J Psychiatry 174:748–755.
46. Abbas AI, Hedlund PB, Huang XP, Tran TB, Meltzer HY, Roth BL (2009): Amisulpride is a potent 5-HT7 antagonist: relevance for antidepressant actions in vivo. Psychopharmacology 205:119–128.
47. Robison AJ, Nestler EJ (2011): Transcriptional and epigenetic mechanisms of addiction. Nat Rev Neurosci 12:623.
48. Laviolette SR (2007): Dopamine modulation of emotional processing in cortical and subcortical neural circuits: Evidence for a final common pathway in schizophrenia? Schizophr Bull 33:971–981.